Computer Vision and Image Understanding 140 (2015) 21–29

Contents lists available at ScienceDirect

Computer Vision and Image Understanding

journal homepage: www.elsevier.com/locate/cviu

Spectral gradient fields embedding for nonrigid shape matching

Alon Shtern*, Ron Kimmel

Geometric Image Processing Laboratory, Technion – Israel Institute of Technologies, Haifa 32000, Israel

ARTICLE INFO

Article history:
Received 15 August 2014
Accepted 9 February 2015

Keywords:
Correspondence
Laplace–Beltrami operator
Shape embedding

ABSTRACT

A popular approach for finding the correspondence between two nonrigid shapes is to embed their two-dimensional surfaces into some common Euclidean space, defining the comparison task as a problem of rigid matching in that space. We propose to extend this line of thought and introduce a novel spectral embedding, which exploits gradient fields for point to point matching. With this new embedding, a fully automatic system for finding the correspondence between shapes is introduced. The method is demonstrated to accurately recover the natural maps between nearly isometric surfaces and shown to achieve state-of-the-art results on known shape matching benchmarks.

1. Introduction

The embedding of manifolds into some Euclidean space is often used for simplifying matching and comparison procedures [1–3]. A useful property of such a target metric space is that corresponding points of different isometric shapes are mapped to nearby points in the target space. In that case, the embedding of multiple isometric shapes into this common target space naturally leads to a distance between shapes that is easy to compute. Recently, attention has been given to the spectral type of embedding that use the eigenvalues and eigenfunctions of the Laplace–Beltrami operator of the shape as a target space [2,4–6]. The fact that the Laplace–Beltrami operator is invariant to isometric deformations makes spectral embedding well suited for comparing the same object in different poses and expressions.

Bérard et al. [1] exhibited the spectral embedding of Riemannian manifolds by their heat kernel. They embedded manifolds into a compatible common target space (infinite Hilbert space) and used the Hausdorff distance in that space to define a metric between isometry equivalent classes of Riemannian manifolds. It means, in particular, that two manifolds are at zero distance if and only if they are isometric.

Rustamov [4] introduced the *global point signature* (GPS) of a point on a shape. It encodes both the eigenvalues and the eigenfunctions of the Laplace–Beltrami operator evaluated at that point. The GPS kernel is, in essence, the integration over all scales of the heat kernel on the surface [7]. The GPS kernel coincides with the Green's function, and in some sense measures the extent to which two points are geometrically connected. He showed that the GPS embedding of a surface without self-intersections has no self-intersections as well.

A different approach was introduced by Sun et al. [5] Their signature, called the *heat kernel signature* (HKS), is defined for every point of the shape, by observing the heat kernel in that point over time. The set of all HKS on a shape characterizes a given surface up to an isometry under the condition that the eigenvalues of the Laplace–Beltrami operator are non-repeating. The invariance of the heat kernel signature to isometric deformations ensures that this signature can be used to find correspondence between different poses of the same shape.

We propose a novel spectral embedding, using gradient fields (GFs) of the Laplace–Beltrami operator eigenfunctions, for correspondence detection. We call the gradient fields of the eigenfunctions, *spectral gradient fields* (or spectral GFs), and refer to the proposed embedding as the *spectral gradient fields embedding*. As Laplace–Beltrami eigenfunctions computed independently for different shapes are often incompatible with each other, the aim of our construction is to embed the shapes using the eigenfunctions that correspond to the lowest eigenvalues. While existing methods [1,4] use the eigenfunctions themselves to define the target space, we embed the shapes using pairs of eigenfunctions. Thereby, more information is being extracted from the interaction between the relatively stable first few eigenfunctions.

1.1. Contribution

We propose to find correspondence by embedding the shapes using a point-wise feature vector, which is based on the inner and external products between the GFs of pairs of eigenfunctions.

* Corresponding author.
E-mail addresses: ashtern@tx.technion.ac.il (A. Shtern), ron@cs.technion.ac.il (R. Kimmel).

http://dx.doi.org/10.1016/j.cviu.2015.02.004
1077-3142/

For each pair of eigenfunctions ϕ_i, ϕ_j, that correspond to the eigenvalues λ_i, λ_j, we calculate their respective gradient fields $\nabla\phi_i, \nabla\phi_j$, and compute the inner product $\langle \nabla\phi_i, \nabla\phi_j \rangle$, and the external product taken as the cross product in the normal direction $((\nabla\phi_i \times \nabla\phi_j) \cdot \mathbf{n})$. Fig. 1 presents two eigenfunctions and their corresponding spectral GFs inner and external products. Because the inner and external products depend on the eigenfunctions and the gradient operator, they are relatively stable under isometric deformations, different poses and articulations. These features enable us to extract fine geometric information from a pair of eigenfunctions, as well as obtaining the global structure of an object. For the human shape shown as an example in Fig. 1, the inner product (third column and enlarged figure) distinguishes between the neck's left and right sides, while the external product (fourth column) partitions the body's front and back.

The proposed feature vector defines an embedding of shapes into Euclidean space. To the best of our knowledge, this is the first time that spectral gradient fields are used for such an embedding (see Table 1 for a summary of existing embedding methods). We prove that the proposed spectral gradient fields embedding is injective. Therefore, it naturally induces a distance function between any two points on the surface. In this metric space a distance between shapes is relatively simple to compute. We define such a distance measure, which we refer to as the *spectral gradient fields distance*, in a way similar to the definition of the spectral embedding distance defined by Bérard et al. [1]. In the classic spectral embedding, the target space is described by the eigenfunctions of the Laplace–Beltrami operator. In the proposed target space, we embed the shapes into a much richer space, by using the conformal-based inner product between GFs of the eigenfunctions [8]. We describe the properties of the proposed distance measure, and prove that it is a pseudometric.

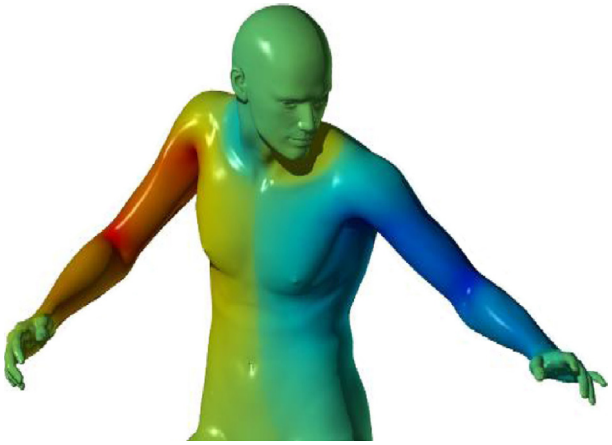

1.2. Metric geometry

A metric space (X, d_X) is a pair, where X is a set and $d_X : X \times X \to \mathbb{R}_{\geq 0}$ is a well defined distance function, satisfying the symmetry property $d_X(x_1, x_2) = d_X(x_2, x_1)$, the identity property $d_X(x_1, x_2) = 0$ iff $x_1 = x_2$, and the triangle inequality $d_X(x_1, x_3) \leq d_X(x_1, x_2) + d_X(x_2, x_3)$ for any $x_1, x_3 \in X$. If the distance $d_X(x_1, x_2)$ between two distinct points can be zero, then (X, d_X) is called a pseudometric space.

Suppose $A, B \in X$ are two closed subsets of a common bigger metric space (X, d_X), and we want to compare A to B in order to decide whether they represent the same object or not, one might compute the Hausdorff distance $d_{\mathcal{H}}(A, B)$ between A and B

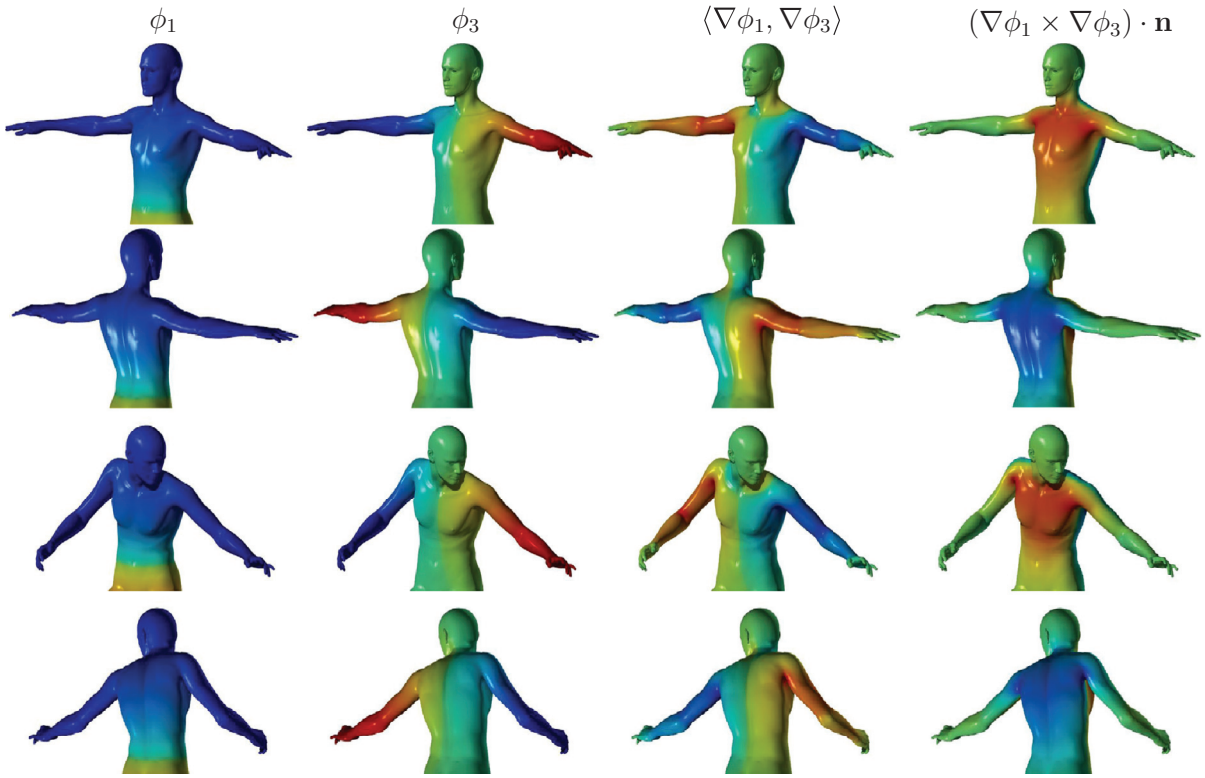

Fig. 1. Inner and external products of the gradient fields of a pair of eigenfunctions ϕ_1, ϕ_3. The inner product (third column, and enlarged figure) exhibits finer details of the neck and hands of the human shape. Notice in the forth column, that the difference between front and back is captured by the external product. In the last two rows we see that these features are stable under a natural pose of the articulated object. In all our figures, red and blue colors represent high and low values of scalar functions on the shapes.

Table 1
The spectral gradient fields embedding and other known spectral embeddings and signatures.

Spectral gradient fields	$(\sqrt{\lambda_i\lambda_j})^{-1}\langle\nabla\phi_i(x),\nabla\phi_j(x)\rangle$, $(\sqrt{\lambda_i\lambda_j})^{-1}((\nabla\phi_i(x)\times\nabla\phi_j(x))\cdot\mathbf{n}(x))$; $i,\ j\geq 1$
Spectral embedding [1]	$e^{-\lambda_i t}\phi_i(x)$; $i\geq 1, t>0$
Global point signature [4]	$(\sqrt{\lambda_i})^{-1}\phi_i(x)$; $i\geq 1$
Heat kernel signature [5]	$\sum_k \exp(-\lambda_k t)\phi_k^2(x)$; $t>0$

$$d_{\mathcal{H}}(A,B)\equiv\max\left(\sup_{a\in A}\inf_{b\in B}d_X(a,b),\sup_{b\in B}\inf_{a\in A}d_X(a,b)\right),$$

and designate two objects $A, B\in X$ as being identical, if $d_{\mathcal{H}}(A,B)=0$.

A different approach to compare objects, is to treat them as metric spaces, and check if these metric spaces are isometric or not. We say the metric spaces (X,d_X) and (Y,d_Y) are isometric when there exists a bijective mapping $\varphi: X\to Y$ such that $d_X(x_1,x_2)=d_Y(\varphi(x_1),\varphi(x_2))$ for all $x_1,\in X$. Such a φ is an isometry between (X,d_X) and (Y,dY). In other words, an isometry between two shapes is a map between their two dimensional surfaces that preserves the distances between any two points.

For example, when considering shapes as two-dimensional Riemannian manifolds embedded in the three dimensional Euclidean space, and if one is interested in invariance to deformations of a surface that preserve the geodesic metric, then the surfaces can be treated as metric spaces equipped with the geodesic distances of the Riemannian manifold [9,10].

1.3. The gradient and the Laplace–Beltrami operator

Let X be a Riemannian manifold. For any smooth function $f: X\to\mathbb{R}$ the gradient of f is the vector field ∇f defined through the Riemannian manifold's inner product, such that for any vector field U,

$$\langle\nabla f(x),U(x)\rangle=\partial_U f(x),$$

where $\partial_U f(x)$ is the directional derivative of f at $x\in X$, in the direction $U(x)$.

The Laplace–Beltrami operator, denoted by Δ, is the divergence of the gradient

$$\Delta f\equiv\operatorname{div}\operatorname{grad} f,$$

and can be considered as a generalization of the standard notion of the Laplace operator to compact Riemannian manifolds [11–13]. The Laplace–Beltrami operator is invariant to geodesic-preserving deformations because it is defined in terms of the surface metric tensor which is isometry invariant.

The eigendecomposition of $-\Delta$ consists of nonnegative eigenvalues $0=\lambda_0<\lambda_1\leq\cdots\leq\lambda_i\leq\cdots$, satisfying

$$-\Delta\phi_i\equiv\lambda_i\phi_i.$$

The set of corresponding eigenfunctions given by

$$\Phi\equiv\{\phi_0,\phi_1,\ldots,\phi_i,\ldots\},$$

forms an orthonormal eigenbasis, such that $\int_X\phi_i(x)\phi_j(x)d\mathrm{V}=\delta_{ij}$, where $d\mathrm{V}$ is the volume element on the manifold X.

1.4. Spectral embedding

Bérard et al. [1] used the spectral properties of the heat operator $e^{t\Delta}$ to define a metric between two Riemannian manifolds $X, Y\in\mathcal{M}$. Here, $\mathcal{M}$ is the set of all closed (i.e. compact without boundary) Riemannian manifolds of dimension n. Given a Riemannian manifold $X\in\mathcal{M}$ with volume $\mathrm{Vol}(X)$ and some $t>0$, they based their metric on the eigendecomposition of the heat kernel and defined the spectral embedding $I_t^{\Phi}: X\to\ell^2$ from the Riemannian manifold X into the Hilbert space ℓ^2 of real valued square-summable sequences

$$I_t^{\Phi}(x)\equiv\left\{\sqrt{\mathrm{Vol}(X)}e^{-\lambda_i t/2}\phi_i(x)\right\}_{i\geq 1},$$

utilizing the eigenfunctions ϕ_i and eigenvalues λ_i of the Laplace–Beltrami operator Δ.

Given a pair of eigenbases Φ^X,Φ^Y, they embedded the two Riemannian manifolds X and Y into $I_t^{\Phi^X}$ and $I_t^{\Phi^Y}$, respectively. Then, they measured the Hausdorff distance $d_{\mathcal{H}}$ between the manifolds in the common ℓ^2 space. Bérard et al. defined the distance $d_t^{\mathrm{EMB}}:\mathcal{M}\times\mathcal{M}\to\mathbb{R}_{\geq 0}$ between the manifolds X, Y, as the upper-bound of the Hausdorff distance between any eigenbasis Φ^X and its closest counterpart Φ^Y.

$$d_t^{\mathrm{EMB}}(X,Y)\equiv\max(d_{l_t}(X,Y),d_{l_t}(Y,X)),$$
$$d_{l_t}(X,Y)\equiv\sup_{\{\Phi^X\}}\inf_{\{\Phi^Y\}}d_{\mathcal{H}}(I_t^{\Phi^X},I_t^{\Phi^Y}).$$

We call $d_t^{\mathrm{EMB}}(X,Y)$ the *spectral embedding distance* (for a detailed description of the spectral embedding distance, we refer the reader to [1]). They showed that for any fixed $t>0$, the spectral embedding distance d_t^{EMB} is a metric between isometry classes of Riemannian manifolds. In particular, $d_t^{\mathrm{EMB}}(X,Y)=0$ if and only if the Riemannian manifolds X and Y are isometric.

2. Spectral gradient fields embedding

2.1. Inner and external products

A spectral gradient field is a tangent vector field defined as the gradient of an eigenfunction $\nabla\phi_i$. The feature vector we define is based on the inner product between two spectral gradient fields, $\omega_{i,j}: X\to\mathbb{R}$ for all $i, j\geq 1$, where

$$\omega_{i,j}(x)\equiv\mathrm{Vol}(X)\left(\sqrt{\lambda_i\lambda_j}\right)^{-1}\langle\nabla\phi_i(x),\nabla\phi_j(x)\rangle. \tag{1}$$

For the special case that the Riemannian manifold is an oriented two-dimensional manifold embedded in $\mathbb{R}^3$, we enrich the feature vector by using the cross product between two spectral GFs in the normal direction, $\nu_{i,j}: X\to\mathbb{R}$ for all $i, j\geq 1$, where

$$\nu_{i,j}(x)\equiv\mathrm{Vol}(X)\left(\sqrt{\lambda_i\lambda_j}\right)^{-1}((\nabla\phi_i(x)\times\nabla\phi_j(x))\cdot\mathbf{n}(x)). \tag{2}$$

2.2. Embedding

Let us study the embedding and the distance between shapes that are induced by this feature vector. We limit our analysis to the inner product between the gradients of the eigenfunctions. Thus, we define the *spectral GFs embedding* $J_t^{\Phi}: X\to\ell^2$ as

$$J_t^{\Phi}(x)\equiv\{e^{-(\lambda_i+\lambda_j)t/2}\omega_{i,j}(x)\}_{i,j\geq 1},\quad t>0.$$

Proposition 1. *Let $x_1,\in X$ be two distinct points on the Riemannian manifold $X\in\mathcal{M}$. Then, there exists a smooth function f, such that $\nabla f(x_1)\neq 0$, and $\nabla f(x_2)=0$.*

The proof of Proposition 1 is given in A.

Theorem 1. *For a Riemannian manifold $X\in\mathcal{M}$, the embedding $J_t^{\Phi}: X\to\ell^2$ is injective, i.e. $x_1\neq x_2\Leftrightarrow J_t^{\Phi}(x_1)\neq J_t^{\Phi}(x_2)$.*

Proof. The proof is motivated by Rustamov's analysis of his GPS embedding [4]. Suppose that for two different points $x_1, \in X$, we have $J_t^\Phi(x_1) = J_t^\Phi(x_2)$. This means that for all $i, j \geq 1$, we have $\langle \nabla\phi_i(x_1), \nabla\phi_j(x_1)\rangle = \langle \nabla\phi_i(x_2), \nabla\phi_j(x_2)\rangle$. Now, any smooth scalar function $f : X \to \mathbb{R}$ can be represented as a linear combination of the eigenbasis $f = \sum_i a_i\phi_i$. We can thereby write the norm of the gradient as

$$\|\nabla f(x_1)\|^2 = \sum_{i,j} a_i a_j \langle \nabla\phi_i(x_1), \nabla\phi_j(x_1)\rangle = \sum_{i,j} a_i a_j \langle \nabla\phi_i(x_2), \nabla\phi_j(x_2)\rangle = \|\nabla f(x_2)\|^2.$$

On the other hand, using Proposition 1, there always exists a smooth function f, such that $\|\nabla f(x_1)\| \neq \|\nabla f(x_2)\|$, a contradiction. Therefore, $J_t^\Phi(x_1) \neq J_t^\Phi(x_2)$. □

Theorem 2. *The family of maps $\{J_t^\Phi\}_{t>0}$ is invariant to global scaling of the metric.*

See Appendix B for a proof of this Theorem.

2.3. Point to point distance

Given a Riemannian manifold $X \in \mathcal{M}$, the embedding $J_t^\Phi : X \to \ell^2$ induces a metric $\tilde{d}_X : X \times X \to \mathbb{R}_{\geq 0}$ on the manifold, in a way that the distance between any two points $x_1, \in X$ coincides with the distance between the images of these points in the ℓ^2 space

$$\tilde{d}_X(x_1, x_2) \equiv \|J_t^\Phi(x_1) - J_t^\Phi(x_2)\|_{\ell^2}.$$

The metric $\tilde{d}_X(x_1, x_2)$ is a well defined distance function which is invariant to the choice of the orthonormal eigenbasis Φ.

2.4. Distance between Riemannian manifolds

Let $X, Y \in \mathcal{M}$ be the two closed Riemannian manifolds we would like to compare, and let us be given some $t > 0$. Given a pair of eigenbases Φ^X, Φ^Y, we embed the two Riemannian manifolds X and Y into $J_t^{\Phi^X}$ and $J_t^{\Phi^Y}$, respectively, and measure the *Hausdorff distance* $d_{\mathcal{H}}$ between the manifolds in the common ℓ^2 space. We define the *spectral gradient fields distance*, denoted by $d_t^{\mathrm{GF}} : \mathcal{M} \times \mathcal{M} \to \mathbb{R}_{\geq 0}$, as the supremum of the Hausdorff distance between any eigenbasis Φ^X and its closest counterpart Φ^Y.

$$d_t^{\mathrm{GF}}(X, Y) \equiv \max(d_{J_t}(X, Y), d_{J_t}(Y, X)),$$

$$d_{J_t}(X, Y) \equiv \sup_{\{\Phi^X\}} \inf_{\{\Phi^Y\}} d_{\mathcal{H}}(J_t^{\Phi^X}, J_t^{\Phi^Y}).$$

We say that X, Y are *spectral gradient fields equivalent*, if the metric spaces $(X, \tilde{d}_X)$, $(Y, \tilde{d}_Y)$ are isometric and if $d_t^{\mathrm{GF}}(X, Y) = 0$.

Theorem 3. *The spectral GFs distance d_t^{GF} is a pseudometric between spectral GFs equivalent classes of Riemannian manifolds.*

The proof of Theorem 3 is given in C.

Remark. The use of the spectral GFs external product $((\nabla\phi_i \times \nabla\phi_j) \cdot \mathbf{n}(x))$ is obviously restricted to oriented two-dimensional surfaces embedded in the three-dimensional Euclidean space. Although the cross product of two tangent vectors is extrinsic in nature, its projection in the normal direction is invariant to isometric deformations. Consequently, for a two-dimensional surface embedded in $\mathbb{R}^3$, adding the elements $e^{-(\lambda_i^X + \lambda_j^Y)t/2}\nu_{i,j}$ for all $i, j \geq 1$ to the embedding J_t^Φ, leaves the above analysis unchanged. Hence, the statements of Theorems 1–3 hold for the extended feature vector as well.

Conjecture 1. The spectral GFs distance d_t^{GF} is a metric between spectral GFs equivalent classes of Riemannian manifolds.

We consider Conjecture 1 in C. We believe that a proof of this conjecture is beyond the scope of this paper and leave it to future work.

3. Experiments and results

3.1. Truncated feature vector

Let us study the spectral GFs feature vector when we are restricted to using the N_0 eigenfunctions that correspond to the lowest eigenvalues. Remember that we are driven by the task of finding correspondence between two nearly isometric shapes. Because empirical evidence suggests that there are only a few eigenfunctions that are stable to approximately isometric deformations, for the shape matching application we prefer to avoid eigenfunctions that correspond to high eigenvalues.

In our analysis (and implementation) we use the plain vanilla feature vector $J^\Phi \equiv J_\omega^\Phi \cup J_\nu^\Phi$, where $J_\omega^\Phi \equiv \{\omega_{i,j}\}_{1\leq i\leq j\leq N_0}$ and $J_\nu^\Phi \equiv \{\nu_{i,j}\}_{1\leq i<j\leq N_0}$ are the inner and external parts of the feature vector, respectively. J^Φ excludes the dependency on the parameter t. This feature vector is invariant to global scaling as shown in the proof of Theorem 2. Notice, that we have omitted some of the features because $\nu_{i,i} = 0$, $\nu_{i,j} = -\nu_{j,i}$ and $\omega_{i,j} = \omega_{j,i}$ for all i, j. In that case, $|J_\omega^\Phi| = \frac{1}{2}N_0(N_0 - 1) + N_0$ and $|J_\nu^\Phi| = \frac{1}{2}N_0(N_0 - 1)$. Therefore, the number of nontrivial and unique features in J^Φ is N_0^2.

3.2. Spectrum

As a case study, we analyze the spectral GFs embedding of a human shape. For this shape, assume we are given $N_0 = 6$ eigenfunctions. Accordingly, the size of the spectral GFs feature vector is $6^2 = 36$. Since J^Φ is nonlinear in ϕ, it is interesting to visualize how the energy of the feature vector is distributed as a function of the eigenvalues. This spectral density $S(\lambda_i)$ is calculated by

$$S(\lambda_i) \equiv \frac{\sum_n \alpha_{n,i}^2}{\sum_{n,i} \alpha_{n,i}^2}, \quad \alpha_{n,i} \equiv \int_X f_n(x)\phi_i(x)da(x),$$

where $f_n(x)$ is the n_{th} element of the feature vector. In Fig. 2, we plot the energy of the spectral GFs features vector as a function of the

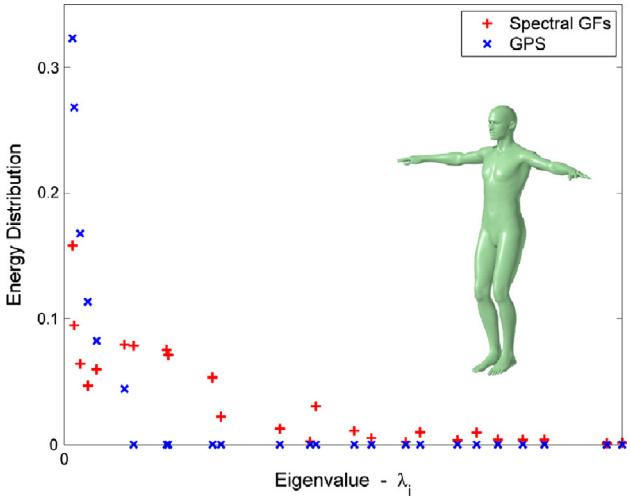

Fig. 2. Spectral density of the spectral GFs feature vector computed on the human shape, compared to the spectrum of the GPS embedding.

eigenvalues, and compare it to the spectrum of the global point signature (GPS) feature vector. We see, that the spectrum of the inner and external products is more widely distributed, which means that they could reflect finer details of the surface structure.

3.3. Intra-shape point to point distances

The feature vector J^{Φ} induces a distance $\tilde{d}_X : X \times X \to \mathbb{R}_{\geq 0}$ between points on the shape

$$\tilde{d}_X(x_1, x_2) \equiv \|J^{\Phi}(x_1) - J^{\Phi}(x_2)\| = \sum_{i,j=1}^{N_0} (\omega_{i,j}(x_1) - \omega_{i,j}(x_2))^2 + (\nu_{i,j}(x_1) - \nu_{i,j}(x))^2.$$

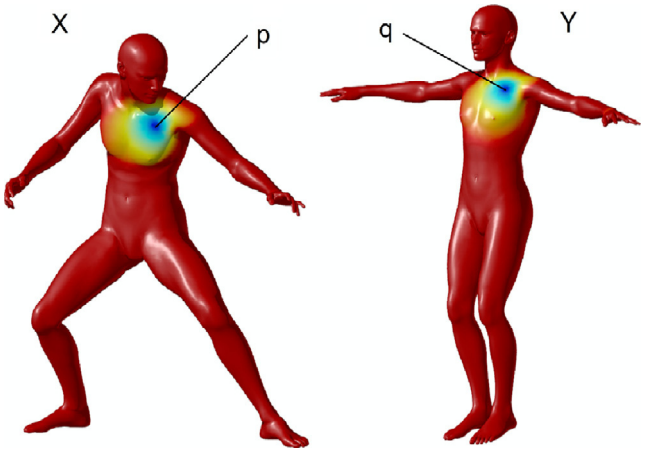

Fig. 3. The spectral GFs feature vector induced the distance function $\tilde{d}_X(p, x)$ between a fixed point p to all points $x \in X$ (left), and the distance function $\tilde{d}_Y(q, y)$ from the corresponding point $q = \varphi(p)$ to all points on shape Y (right).

Fig. 3 depicts the distance function $\tilde{d}_X(p, x)$, between a fixed point $p \in X$ on the front of the human shape to any other point $x \in X$. We observe that $\tilde{d}_X(p, x)$ is invariant to the isometric deformation, as expected.

3.4. Inter-shape point to point distances

For two shapes X, Y, let us assume we are given compatible eigenbases of size N_0, meaning that $\phi_i^X(x) \approx \phi_i^Y(\varphi(x)), \forall i \in \{1 \dots N_0\}$, for all points $x \in X$. In the common embedding space, the distance $d_{X,Y}(x, y) : X \times Y \to \mathbb{R}$ between a point on one shape to a point on the other shape is simply

$$d_{X,Y}(x, y) = \|J^{\Phi^X}(x) - J^{\Phi^Y}(y)\| = \sum_{i,j=1}^{N_0} (\omega_{i,j}^X(x) - \omega_{i,j}^Y(y))^2 + (\nu_{i,j}^X(x) - \nu_{i,j}^Y(y))^2. \quad (3)$$

In Fig. 4 we visualize the distance $d_{X,Y}(p, y)$ from the fixed point $p \in X$ to all points $y \in Y$. We see (column 1), that points on surface Y that are close to the image of p, also have low values of $\tilde{d}_{X,Y}(p, y)$. Hence, for a point to point correspondence application, we should assign the corresponding point of p as the one with the smallest distance from p, in the common Euclidean space. Notice especially, that while the GPS embedding (column 4) makes points on the back mistakenly close to p, by using the spectral GFs feature vector this effect is diminished. This can be explained by the use of the $\nu_{i,j}$ features (column 3), that include the cross product operation which is an extrinsic operation. Pure intrinsic embeddings do not use this important attribute of the surface, so the embedding J_{ν}^{Φ} presents additional global features. Combined with the inner product based embedding J_{ω}^{Φ} which is more locally accurate (column 2), the spectral gradient fields embedding J^{Φ} is well suited for finding point to point correspondences.

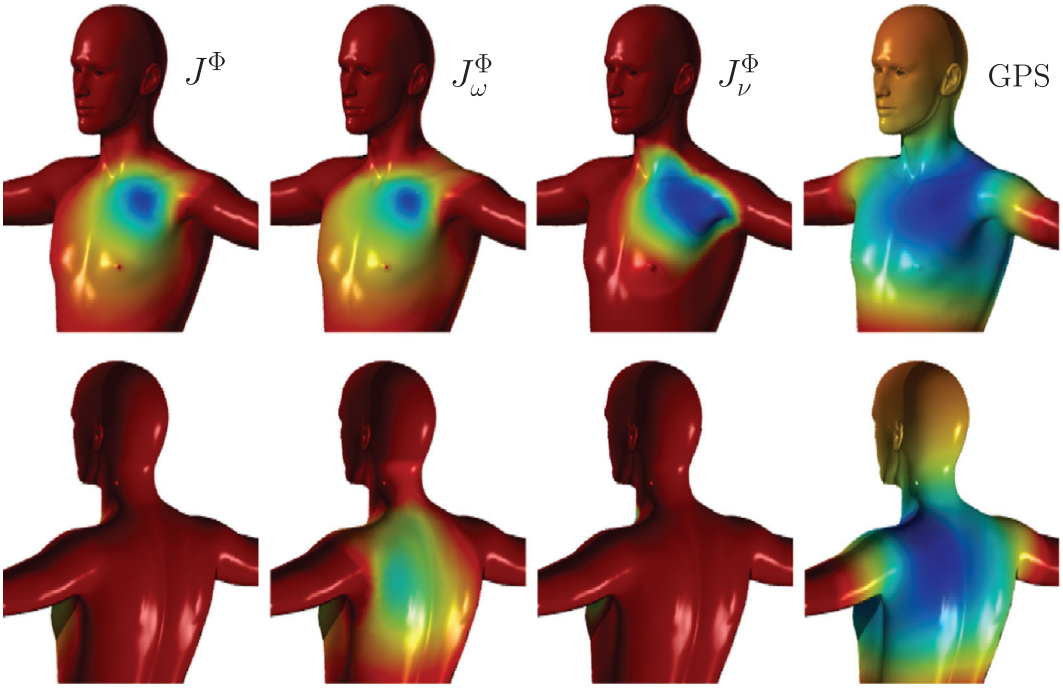

Fig. 4. In the common space, the inter-shape distance $d_{X,Y}(p, y)$, is calculated between a fixed point p on shape X and all points in shape Y. From left to right: spectral GFs with the embeddings J^{Φ}, J_{ω}^{Φ} (inner-products), J_{ν}^{Φ} (external products) and the GPS embedding.

3.5. Compatible eigenfunctions

For two nearly isometric shapes X, Y, one might say that the eigenfunction ϕ_i^X is matched to the eigenfunction ϕ_j^Y up to a sign, if the difference between ϕ_i^X and $\phi_j^Y \circ \varphi$

$$E(i,j) \equiv \min_{s\in\{+1,-1\}} \int_X |\phi_i^X(x) - s\phi_j^Y(\varphi(x))|^2 da(x), \tag{4}$$

is lower than a certain threshold, where da is the area element of X. In Fig. 5, we see that for the databases we analyze [15,16], the probability of finding a match for the ith eigenfunction drops sharply as i increases beyond a certain point (the seventh eigenfunction for the databases we tested). This means that N_0, the number of eigenfunctions that is used for defining the common embedding, should be kept small.

3.6. Implementation

For the purpose of testing our ideas, we developed a holistic correspondence system. At the heart of the system we use the spectral GFs embedding, defined in Eqs. (1) and (2), and compute the inter-shape point to point distances $d_{X,Y}(x,y)$ of Eq. (3), where we use $N_0 = 6$ compatible eigenfunctions that are found automatically (based on [17]). Then, we apply a nearest neighbor search to find the initial correspondence

$$\hat{\varphi}_0(x) = \operatorname*{argmin}_{y\in Y} d_{X,Y}(x,y). \tag{5}$$

As a preprocess step, pairs of points that have low possibility of being matched are filtered out by comparing a mix of global and local features, using the compatible eigenfunctions themselves and the wave kernel signature [6]. We filter out pairs of points if their feature vectors are too far in the L^2 sense. After applying the spectral GFs embedding method using Eq. (5), we refine the correspondence with the *iterative closest spectral kernel maps* (ICSKM) algorithm [18]. The alignment of the spectral kernels of the two shapes by the ICSKM algorithm, produces the final dense map $\hat{\varphi} : X \to Y$.

3.7. Performance

We tested the proposed method on pairs of shapes represented by triangulated meshes from both the SCAPE database [15] and the TOSCA database [16]. The SCAPE dataset contains 71 registered meshes of a particular person in different poses. The TOSCA dataset contains 80 densely sampled synthetic human and animal surfaces, divided into several classes with given ground-truth point-to-point correspondences between the shapes within each class. We compare the results of our framework to several correspondence detection methods.

- Spectral GFs Embedding – the method proposed in this paper.
- Spectral Maps – the correspondence system used in this paper, without the use of the spectral GFs embedding. At the preprocess stage we filter out all correspondences except one.
- Blended – the method proposed by Kim et al. that uses a weighted combination of isometric maps [14].

Figs. 6 and 7 compare our correspondence method with existing methods on the SCAPE and TOSCA benchmarks, using the evaluation protocol proposed in [14]. For each method we plot the distortion curves with the ICSKM refinement procedure (solid), and without it (dotted). The distortion curves describe the

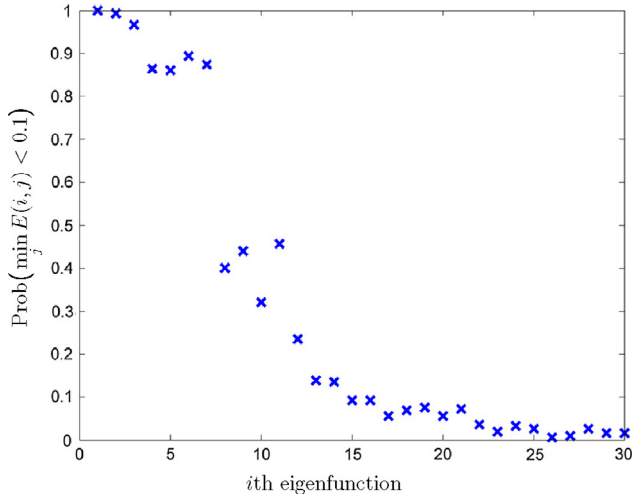

Fig. 5. The empirical probability that there is an eigenfunction ϕ_j^Y that matches ϕ_i^X up to a sign. The matching threshold is set to 0.1, i.e. we check if $E(i,j) < 0.1$ for some j (see Eq. (4)). Notice, that this probability drops sharply beyond the seventh eigenfunction.

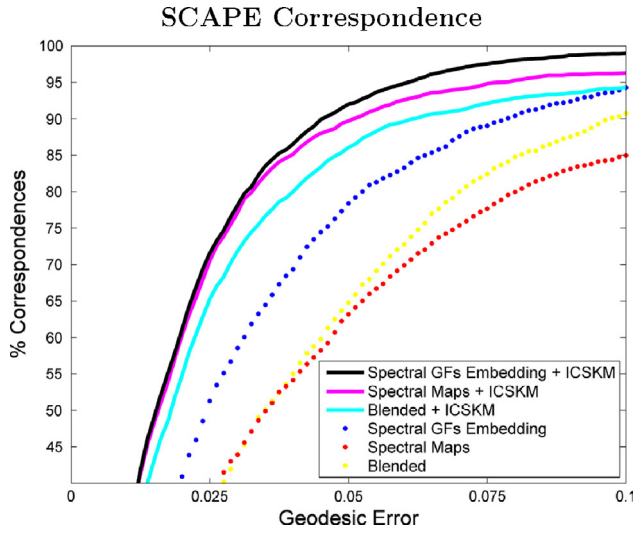

Fig. 6. Evaluation of the correspondence system applied to shapes from the SCAPE database, using the protocol of [14], (with allowed symmetries).

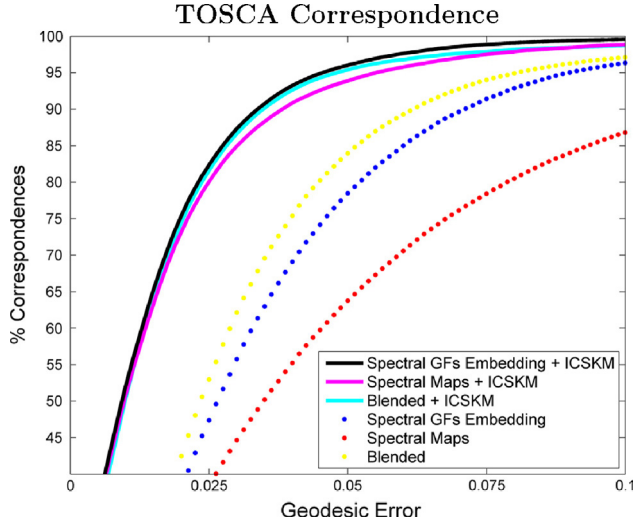

Fig. 7. Evaluation of the correspondence system applied to shapes from the TOSCA database, using the protocol of [14].

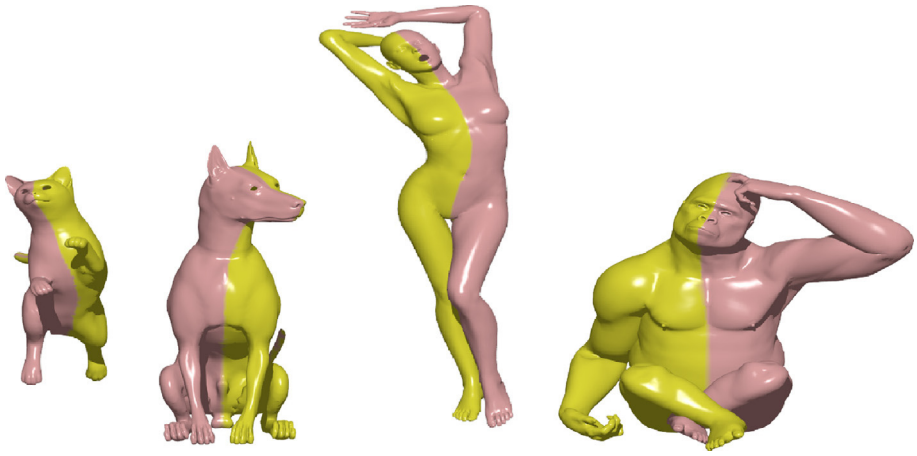

Fig. 8. Bilateral symmetry. The two mirror halves of several shapes from the TOSCA database are found by embedding the shape using spectral gradient fields.

percentage of surface points falling within a relative geodesic distance from what is assumed to be their true locations. For each shape, the geodesic distance is normalized by the square root of the shape's area. It is evident from the benchmarks that the proposed method is well suited for finding maps between approximately isometric shapes, and together with the ICSKM algorithm achieves state-of-the-art results.

3.8. Reflective symmetry

Intrinsic symmetry detection can be viewed as finding a map from a shape to itself [19]. When the shape has a reflective symmetry, its self-map flips the orientation of the surface. In that case, we can apply the proposed shape matching method, by adjusting the normal to the surface to point inward, and consequently change the external product features of the reflective shape to be $-\nu_{i,j}$. Then, we can use the estimated reflective self-map $\hat{\varphi}_R : X \to X$ to partition the shape into its two mirror halves. First, we find a point p that is well inside one of the two halves of the shape, for example by selecting a point that is as far as possible from its reflective image $\hat{\varphi}(p)$, i.e. we find the point $p = \text{argmax}_{x\in X} g(x, \hat{\varphi}_R(x))$, where $g : X \times X \to \mathbb{R}_{\geq 0}$ is the geodesic distance function between two points on the surface of the shape. Then, we check if each point $x \in X$ belongs to the half of the shape that includes p. We assign x to this half if $g(x, p) + g(\hat{\varphi}_R(x), \hat{\varphi}_R(p))$ is less than $g(\hat{\varphi}_R(x), p) + g(x, \hat{\varphi}_R(p))$. In Fig. 8, we demonstrate the effectiveness of the proposed approach, by visualizing the bilateral symmetry for several shapes from the TOSCA database.

4. Conclusions

A new feature vector for embedding nonrigid shapes was introduced and integrated into a holistic shape matching system. The embedding, which is proved to be injective, induces a distance between points on the surface, and can be defined to measure a distance between shapes. We have demonstrated the effectiveness of the proposed approach by achieving state-of-the-art results on shape matching benchmarks.

In the future, we plan to examine the properties of the GFs embedding in conjunction with compatible functions on the two shapes, that are different from the eigenfunctions. For example, one may use the heat kernel signature (HKS), wave kernel signature (WKS) [6] or the heat kernel maps (HKM) [20] set with landmark correspondences. These options seem particularly useful when the shapes are noisy, or the deformations are large, making the eigenfunctions incompatible.

Acknowledgment

This work has been supported by Grant agreement No. 267414 of the European Community's FP7-ERC program.

Appendix A. Proof of Proposition 1

We need to prove that if $x_1,$ are two distinct points on the Riemannian manifold, then, there exists a smooth function f, such that $\nabla f(x_1) \neq 0$, and $\nabla f(x_2) = 0$. We use two technical Lemmas.

Lemma 1. *Let U_1, U_2 be two disjoint closed sets. Then, there exists a smooth function $u_1 : X \to \mathbb{R}_{\geq 0}$, such that*

i. $u_1(x) = 1, \forall x \in U_1$.
ii. $u_1(x) = 0, \forall x \in U_2$.

Proof. U_1, U_2 are disjoint, thereby $\{XU_2, XU_1\}$ is an open cover for X. Hence, there exists a partition of unity of nonnegative functions $u_1, u_2 : X \to \mathbb{R}_{\geq 0}$, such that the support of u_1 is contained in XU_2 and the support of u_2 is contained in XU_1. Moreover, $u_1 + u_2 = 1$ everywhere.

i. The support of u_2 is contained in $XU1$, hence, $u_2(x) = 0, \forall x \in U_1$. Therefore, $u_1(x) = 1 - u_2(x) = 1, \forall x \in U_1$.
ii. Because the support of u_1 is contained in XU_2, it follows that $u_1(x) = 0, \forall x \in U_2$.

Lemma 2. *Let $x_1,$ be two distinct points on the Riemannian manifold. Then, there exists a smooth function $u_1 : X \to \mathbb{R}_{\geq 0}$, such that $u_1(x_1) = 1, u_1(x_2) = 0, \nabla u_1(x_1) = 0$ and $\nabla u_1(x_2) = 0$.*

Proof. Construct two disjoint closed sets U_1, U_2, such that x_1 is in the interior of U_1, and x_2 is in the interior of U_2. Then, use Lemma 2 to make such u_1. □

Now, take a smooth function $g : X \to \mathbb{R}$, with a non zero gradient at point x_1, i.e. $g(x_1) \neq 0$. Using Lemma 2, construct the function $f = u_1 g$. By the chain rule

$$\nabla f(x_1) = u_1(x_1)\nabla g(x_1) + g(x_1)\nabla u_1(x_1) = 1 \cdot \nabla g(x_1) + g(x_1) \cdot 0,$$
$$\nabla f(x_2) = u_1(x_2)\nabla g(x_2) + g(x_2)\nabla u_1(x_2) = 0 \cdot \nabla g(x_2) + g(x_2) \cdot 0.$$

We conclude that $\nabla f(x_1) \neq 0$ and that $\nabla f(x_2) = 0$.

Appendix B. Proof of Theorem 2

Proof. If the Riemannian manifold $\bar{X}$ is obtained by uniformly scaling the metric of the Riemannian manifold X by a factor $\alpha > 0$, then, the eigenvalues of the Laplace–Beltrami operator are scaled according to $\lambda_i^{\bar{X}} = \alpha^{-2}\lambda_i^X$, the corresponding L^2-normalized eigenfunctions become $\phi_i^{\bar{X}} = \alpha^{-1}\phi_i^X$, and the gradient operator reads $\nabla^{\bar{X}} = \alpha^{-1}\nabla^X$. We have

$$\begin{aligned}\omega_{i,j}^{\bar{X}} &= \mathrm{Vol}(\bar{X})\frac{\langle \nabla^{\bar{X}}\phi_i^{\bar{X}}, \nabla^{\bar{X}}\phi_j^{\bar{X}}\rangle}{\sqrt{\lambda_i^{\bar{X}}\lambda_j^{\bar{X}}}}\\ &= \alpha^2\mathrm{Vol}(X)\frac{\langle \alpha^{-1}\nabla^X\alpha^{-1}\phi_i^X, \alpha^{-1}\nabla^X\alpha^{-1}\phi_j^X\rangle}{\sqrt{\alpha^{-2}\lambda_i^X\alpha^{-2}\lambda_j^X}}\\ &= \mathrm{Vol}(X)\frac{\langle \nabla^X\phi_i^X, \nabla^X\phi_j^X\rangle}{\sqrt{\lambda_i^X\lambda_j^X}} = \omega_{i,j}^X,\end{aligned}$$

which means that $\omega_{i,j}^X$ is global scale invariant. Now, if we set $\bar{t} = \alpha^2 t$

$$\begin{aligned}(J_{\bar{t}}^{\Phi^{\bar{X}}})_{i,j} &= e^{-(\lambda_i^{\bar{X}}+\lambda_j^{\bar{X}})\bar{t}/2}\omega_{i,j}^{\bar{X}} = e^{-(\alpha^{-2}\lambda_i^X+\alpha^{-2}\lambda_j^X)\alpha^2 t/2}\omega_{i,j}^X\\ &= e^{-(\lambda_i^X+\lambda_j^X)t/2}\omega_{i,j}^X = (J_t^{\Phi^X})_{i,j}.\end{aligned}$$

Appendix C. Proof of Theorem 3

We would like to show that the spectral gradient fields distance $d_t^{\mathrm{GF}} : \mathcal{M}\times\mathcal{M} \to \mathbb{R}_{\geq 0}$ satisfies the following properties of a pseudo-metric.

P1: Symmetry – $d_t^{\mathrm{GF}}(X,Y) = d_t^{\mathrm{GF}}(Y,X)$ for every $X, Y \in \mathcal{M}$.
P2: Triangle-inequality – For every three Riemannian manifolds $X, Y, Z \in \mathcal{M}$,

$$d_t^{\mathrm{GF}}(X,Z) \leq d_t^{\mathrm{GF}}(X,Y) + d_t^{\mathrm{GF}}(Y,Z).$$

P3: Identity – If $X, Y \in \mathcal{M}$ are spectral GFs equivalent, then $d_t^{GF}(X,Y) = 0$.

Proposition 2. *For every three Riemannian manifolds $X, Y, Z \in \mathcal{M}$,*

$$d_t^{\mathrm{GF}}(X,Z) \leq d_t^{\mathrm{GF}}(X,Y) + d_t^{\mathrm{GF}}(Y,Z).$$

Proof. We denote

$$\begin{aligned}&d_{X,Y}(x,y) \equiv \|J_t^{\Phi^X}(x) - J_t^{\Phi^Y}(y)\|,\\ &\mathrm{dis}(\varphi) \equiv \sup_{x\in X} d_{X,Y}(x,\varphi(x)),\\ &\mathrm{dis}(\psi) \equiv \sup_{y\in Y} d_{X,Y}(\psi(y),y).\end{aligned}$$

The Hausdorff distance between $J_t^{\Phi^X}$ and $J_t^{\Phi^Y}$ is

$$d_{\mathcal{H}}(J_t^{\Phi^X}, J_t^{\Phi^Y}) = \max\left(\sup_{x\in X}\inf_{y\in Y} d_{X,Y}(x,y), \sup_{y\in Y}\inf_{x\in X} d_{X,Y}(x,y)\right).$$

Lemma 3. *if $d_{\mathcal{H}} = \epsilon$, then there exist $\varphi : X \to Y$ and $\psi : Y \to X$ such that $d_{X,Y}(x,\varphi(x)) \leq \epsilon, \forall x \in X$ and $d_{X,Y}(\psi(y),y) \leq \epsilon, \forall y \in Y$.*

Proof. $X, Y \in \mathcal{M}$ are compact and $J_t^{\Phi^X}, J_t^{\Phi^Y}$ are continuous one-to-one mappings. Thus, their images are also compact, which allows us to define $\varphi(x) = \mathrm{argmin}_{y\in Y} d_{X,Y}(x,y)$ and $\psi(y) = \mathrm{argmin}_{x\in X} d_{X,Y}(x,y)$. □

Now, if $d_t^{\mathrm{GF}}(X,Y) \leq \epsilon$, then, for any Φ^X, one can find Φ^Y, φ, ψ (using Lemma 3) such that $\mathrm{dis}(\varphi) \leq \epsilon$, $\mathrm{dis}(\psi) \leq \epsilon$, i.e.

$$\begin{aligned}&d_{X,Y}(x,\varphi(x)) \leq \epsilon, \forall x,\\ &d_{X,Y}(\psi(y),y) \leq \epsilon, \forall y.\end{aligned}$$

Let $d_t^{\mathrm{GF}}(X,Y) = \epsilon_1$ and $d_t^{\mathrm{GF}}(Y,Z) = \epsilon_2$. Hence, for any Φ^X, there exist two eigenbases (Φ^Y, Φ^Z), and two pairs of corresponding mappings $(\varphi_1 : X \to Y, \psi_1 : Y \to X)$ and $(\varphi_2 : Y \to Z, \psi_2 : Z \to Y)$ satisfying $\mathrm{dis}(\varphi_1) \leq \epsilon_1$, $\mathrm{dis}(\psi_1) \leq \epsilon_1$, and $\mathrm{dis}(\varphi_2) \leq \epsilon_2$, $\mathrm{dis}(\psi_2) \leq \epsilon_2$. Denote by $\varphi = \varphi_2 \circ \varphi_1 : X \to Z$, $\psi = \psi_1 \circ \psi_2 : Z \to X$. Invoking the triangle inequality for ℓ^2 spaces, one has

$$\begin{aligned}d_{X,Z}(x,\varphi(x)) &\leq d_{X,Y}(x,\varphi_1(x)) + d_{Y,Z}(\varphi_1(x),\varphi(x))\\ &\leq \mathrm{dis}(\varphi_1) + \mathrm{dis}(\varphi_2) \leq \epsilon_1 + \epsilon_2, \forall x \in X,\\ d_{X,Z}(\psi(z),z) &\leq d_{X,Y}(\psi(z),\psi_1(z)) + d_{Y,Z}(\psi_2(z),z)\\ &\leq \mathrm{dis}(\psi_1) + \mathrm{dis}(\psi_2) \leq \epsilon_1 + \epsilon_2, \forall z \in Z.\end{aligned}$$

This means that for any Φ^X, we can find Φ^Z, φ, ψ, such that $d_{X,Z}(x,\varphi(x))$ and $d_{X,Z}(\psi(z),z)$ are bounded by $\epsilon_1 + \epsilon_2$. Consequently,

$$\inf_{\{\Phi^Z\}} d_{\mathcal{H}}(J_t^{\Phi^X}, J_t^{\Phi^Z}) \leq \epsilon_1 + \epsilon_2, \forall \Phi^X.$$

Clearly,

$$d_{J_t}(X,Z) = \sup_{\{\Phi^X\}}\inf_{\{\Phi^Z\}} d_{\mathcal{H}}(J_t^{\Phi^X}, J_t^{\Phi^Z}) \leq \epsilon_1 + \epsilon_2.$$

In the same way $d_{J_t}(Z,X) \leq \epsilon_1 + \epsilon_2$, implying $d_t^{\mathrm{GF}}(X,Z) \leq \epsilon_1 + \epsilon_2$. □

We conclude that the distance $d_t^{\mathrm{GF}}(X,Y) : \mathcal{M}\times\mathcal{M} \to \mathbb{R}_{\geq 0}$ satisfies the properties of Theorem 3.

P1: Symmetry – by definition, the function $d_t^{\mathrm{GF}}(X,Y)$ is invariant to permutation of X and Y.
P2: Triangle-inequality – by Proposition 2.
P3: Identity – X, Y cannot be spectral GFs equivalent if $d_t^{\mathrm{GF}}(X,Y) \neq 0$.

Appendix D. Outline of a possible proof of Conjecture 1

Conjecture 1 states that the spectral GFs distance d_t^{GF} is a metric between spectral GFs equivalent classes of Riemannian manifolds. This conjecture can be proved by assuming that $d_t^{GF}(X,Y) = 0$ implies that there exist eigenbases Φ^X, Φ^Y and maps $\varphi : X \to Y$, $\psi : Y \to X$, such that $J_t^{\Phi^X}(x) = J_t^{\Phi^Y}(\varphi(x)), \forall x \in X$ and $J_t^{\Phi^X}(\psi(y)) = J_t^{\Phi^Y}(y), \forall y \in Y$.

Remark. To prove this assumption we suggest to follow the footsteps of Bérard et al. [1], but a rigorous proof of this hypothesis is left for future work.

Now, because $J_t^{\Phi^X}(x) = J_t^{\Phi^Y}(\varphi(x)), \forall x \in X$, then for all $x_1, \in X$ we have

$$\|J_t^{\Phi^X}(x_1) - J_t^{\Phi^X}(x_2)\|_{\ell^2} = \|J_t^{\Phi^Y}(\varphi(x_1)) - J_t^{\Phi^Y}(\varphi(x_2))\|_{\ell^2}.$$

We also know that X, Y are equipped with the metrics $\tilde{d}_X, \tilde{d}_Y$ derived from the distances in the common space

$$\begin{aligned}&\tilde{d}_X(x_1,x_2) = \|J_t^{\Phi^X}(x_1) - J_t^{\Phi^X}(x_2)\|_{\ell^2}, \forall x_1, x_2 \in X,\\ &\tilde{d}_Y(y_1,y_2) = \|J_t^{\Phi^Y}(y_1) - J_t^{\Phi^Y}(y_2)\|_{\ell^2}, \forall y_1, y_2 \in Y.\end{aligned}$$

Hence, φ is a distance preserving map

$$\tilde{d}_X(x_1,x_2) = \tilde{d}_Y(\varphi(x_1),\varphi(x_2)).$$

In the same way

$$\tilde{d}_X(\psi(y_1), \psi(y_2)) = \tilde{d}_Y(y_1, y_2).$$

Moreover, $x = \psi(\varphi(x))$ for all $x \in X$ and $y = \varphi(\psi(y))$ for all $y \in Y$, or else w.l.g.o. there would be two distinct points $x_1, \in X$ such that $x_2 = \psi(\varphi(x_1))$. In that case $J_t^{\Phi^X}(x_1)$ and $J_t^{\Phi^X}(x_2)$ would both be equal to $J_t^{\Phi^Y}(\varphi(x_1))$, which contradicts the fact that $J_t^{\Phi^X}$ is injective. Therefore, φ, ψ are bijections and distance preserving, hence (if our assumption is true), X, Y are spectral GFs equivalent.

References

[1] P. Bérard, G. Besson, S. Gallot, Embedding Riemannian manifolds by their heat kernel, Geom. Funct. Anal. GAFA 4 (4) (1994) 373–398.

[2] A. Elad, R. Kimmel, On bending invariant signatures for surfaces, IEEE Trans. Pattern Anal. Mach. Intell. 25 (10) (2003) 1285–1295.

[3] R.R. Coifman, S. Lafon, A.B. Lee, M. Maggioni, B. Nadler, F. Warner, S.W. Zucker, Geometric diffusions as a tool for harmonic analysis and structure definition of data: diffusion maps, Proc. Nat. Acad. Sci. USA 102 (21) (2005) 7426–7431.

[4] R.M. Rustamov, Laplace-Beltrami eigenfunctions for deformation invariant shape representation, in: Proceedings of the Fifth Eurographics Symposium on Geometry Processing, Eurographics Association, 2007, pp. 225–233.

[5] J. Sun, M. Ovsjanikov, L. Guibas, A concise and provably informative multi-scale signature based on heat diffusion, Computer Graphics Forum, vol. 28, Wiley Online Library, 2009, pp. 1383–1392.

[6] M. Aubry, U. Schlickewei, D. Cremers, The wave kernel signature: a quantum mechanical approach to shape analysis, 2011 IEEE International Conference on Computer Vision Workshops (ICCV Workshops), IEEE, 2011, pp. 1626–1633.

[7] M.M. Bronstein, A.M. Bronstein, Shape recognition with spectral distances, IEEE Trans. Pattern Anal. Mach. Intell. 33 (5) (2011) 1065–1071.

[8] R. Rustamov, M. Ovsjanikov, O. Azencot, M. Ben-Chen, F. Chazal, L.J. Guibas, Map-based exploration of intrinsic shape differences and variability, in: ACM Transactions on Graphics (TOG)-SIGGRAPH 2013 Conference Proceedings, vol. 32, 2013.

[9] F. Mémoli, G. Sapiro, A theoretical and computational framework for isometry invariant recognition of point cloud data, Found. Comput. Math. 5 (3) (2005) 313–347.

[10] A.M. Bronstein, M.M. Bronstein, R. Kimmel, Generalized multidimensional scaling: a framework for isometry-invariant partial surface matching, Proc. Nat. Acad. Sci. USA 103 (5) (2006) 1168–1172.

[11] G. Taubin, A signal processing approach to fair surface design, Proceedings of the 22nd Annual Conference on Computer Graphics and Interactive Techniques, ACM, 1995, pp. 351–358.

[12] B. Lévy, Laplace–Beltrami eigenfunctions towards an algorithm that understands geometry, SMI 2006, IEEE International Conference on Shape Modeling and Applications, 2006.

[13] S. Rosenberg, The Laplacian on a Riemannian Manifold: An Introduction to Analysis on Manifolds, vol. 31, Cambridge University Press, 1997.

[14] V.G. Kim, Y. Lipman, T. Funkhouser, Blended intrinsic maps, ACM Transactions on Graphics (TOG), vol. 30, ACM, 2011, p. 79.

[15] D. Anguelov, P. Srinivasan, H.-C. Pang, D. Koller, S. Thrun, J. Davis, The correlated correspondence algorithm for unsupervised registration of nonrigid surfaces, Adv. Neural Inform. Process. Syst. 17 (2005) 33–40.

[16] A.M. Bronstein, M.M. Bronstein, R. Kimmel, Numerical Geometry of Non-Rigid Shapes, Springer, 2008.

[17] A. Shtern, R. Kimmel, Matching the LBO eigenspace of non-rigid shapes via high order statistics, Axioms 3 (3) (2014) 300–319.

[18] A. Shtern, R. Kimmel, Iterative closest spectral kernel maps, International Conference on 3D Vision (3DV2014), IEEE, 2014.

[19] D. Raviv, A.M. Bronstein, M.M. Bronstein, R. Kimmel, Full and partial symmetries of non-rigid shapes, Int. J. Comput. Vis. 89 (1) (2010) 18–39.

[20] M. Ovsjanikov, Q. Mérigot, F. Mémoli, L. Guibas, One point isometric matching with the heat kernel, Computer Graphics Forum, vol. 29, Wiley Online Library, 2010, pp. 1555–1564.